

## Mixing and the *s*-Process in Rotating AGB Stars

Falk Herwig

*Department of Physics and Astronomy, University of Victoria, 3800  
Finnerty Rd, Victoria, BC, V8P 1A1, Canada*

Norbert Langer

*Astronomical Institute, Universiteit Utrecht, P.O. Box 80000, NL-3508  
TA Utrecht, The Netherlands*

Maria Lugaro

*Institute of Astronomy, University of Cambridge, Madingley Road,  
Cambridge CB3 0HA; United Kingdom*

**Abstract.** We model the nucleosynthesis during a radiative interpulse phase of a rotating  $3 M_{\odot}$  Asymptotic Giant Branch (AGB) star. We find an enhanced production of the neutron source species  $^{13}\text{C}$  compared to non-rotating models due to shear mixing of protons and  $^{12}\text{C}$  at the core-envelope interface. We estimate that the resulting total production of heavy elements by slow neutron capture (*s*-process) is too low to account for most observations. This is due to the fact that rotationally induced mixing during the interpulse phase causes a pollution of the  $^{13}\text{C}$  pocket layer with the neutron poison  $^{14}\text{N}$ . As a result we find a maximum neutron exposure of  $\tau_{\text{max}} = 0.04 \text{ mbarn}^{-1}$  in the *s*-process layer of our solar metallicity model with rotation. This is about a factor of 5...10 less than required to reproduce the observed stellar *s*-process abundance patterns. We compare our results with models that include hydrodynamic overshooting mixing, and with simple parametric models including the combined effects of overshooting and mixing in the interpulse. Within the parametric model a range of mixing efficiencies during the interpulse phase correlates with a spread in the *s*-process-efficiency. Such a spread is observed in AGB and post-AGB stars as well as in pre-solar SiC grains.

### 1. Introduction

The *s*-process is characterized by neutron captures that are immediately followed by  $\beta$ -decays. Unstable isotopes involved in the *s*-process path have typical life times of the order of hours; at neutron densities of  $N_n < 10^{10} \text{ cm}^{-3}$  they decay rather than capture another neutron (see Busso et al., 1999, for a general review of the *s*-process). Current models (Gallino et al., 1998; Goriely & Mowlavi, 2000; Lugaro et al., 2003) favour low mass Asymptotic Giant Branch (AGB) stars as the dominant production site for the *s*-process nuclei with mass numbers  $A > 90$ . In evolved AGB stars He-shell burning is periodically unstable and generates thermal pulse (TP) cycles. The main neutron producing reaction is

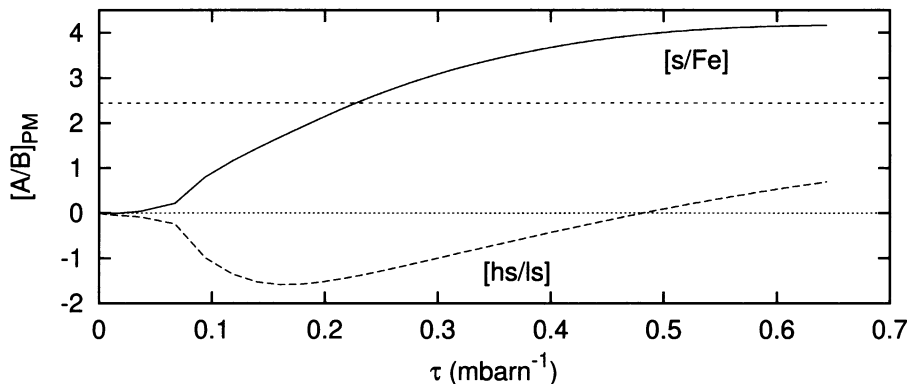


Figure 1.  $s$ -process indices  $[s/Fe]$  and  $[hs/l_s]$  as a function of neutron exposure. As explained in the text this figure translates observational properties of  $s$ -process enriched stars into properties of the partial mixing zone. The dashed/dotted horizontal lines are discussed in the text.

$^{13}C(\alpha, n)^{16}O$  at temperatures as low as  $T = 9 \cdot 10^7$  K. The neutrons are released under radiative conditions during the interpulse phase.

The necessary amount of  $^{13}C$  is produced if protons and  $^{12}C$  can partially mix at the core-envelope interface. This may happen after TP during the dredge-up phase during which a fraction of intershell material is carried into the envelope. The required extra-mixing is still uncertain. With the  $H/^{12}C$ -ratio decreasing continuously from a few hundred in the envelope to zero in the intershell both a  $^{13}C$  as well as a  $^{14}N$  pocket forms. Herwig (2000) has described models with hydrodynamical, diffusive overshooting that leads to a partial mixing zone. However, stars rotate and in this paper we discuss the impact of rotationally induced mixing in AGB star models on the  $s$ -process. A more detailed discussion is available in Herwig et al. (2003).

## 2. Properties of the Partial Mixing Zone

The  $s$ -process abundances observed in AGB stars can be characterized by averaged abundance indicators. The index  $[hs/l_s]$  describes the distribution of the  $s$ -process elements. Stars of solar metallicity show  $-0.5 < [hs/l_s] < 0.0$ , where  $[ls/Fe] = \frac{1}{2}([Y/Fe] + [Zr/Fe])$  and  $hs$  is the average of Ba, La, Nd and Sm. The total overproduction of  $s$ -process elements correlates with the index  $[s/Fe]$ , which is the average of Y and Nd, and observationally  $0 < [s/Fe] < 1$  (Busso et al., 1995).

The observed overproduction factors in the envelope are related to the overproduction factors in the  $s$ -process zone by a number of dilution factors, which result from the subsequent mixing events: the He-flash convective mixing and the third dredge-up. The envelope abundance of any species in the envelope after dredge-up events in  $m$  identical TP cycles is related to the abundance in

the *s*-process zone (partial mixing zone, PM) by

$$Y_{\text{env}} = qmY_{\text{PM}} \frac{M_{\text{PM}}M_{\text{DUP}}}{M_{\text{IS}}M_{\text{env}}} \quad (1)$$

where  $M_{\text{PM}}$ ,  $M_{\text{DUP}}$ ,  $M_{\text{IS}}$  and  $M_{\text{env}}$  are the masses of the partial mixing zone, the dredged up layer, the intershell zone covered by the He-flash convection and the envelope mass respectively. These quantities change with the pulse number, typical numbers in low mass stars are  $M_{\text{DUP}} \sim 3 \cdot 10^{-3} M_{\odot}$ ,  $M_{\text{IS}} \sim 10^{-2} M_{\odot}$  and  $M_{\text{env}} \sim 0.5 M_{\odot}$ . The factor  $q$  describes the effect of the overlapping of the He-flash convection zone in subsequent thermal pulses and can be estimated to be  $q = 2.3$  (see Herwig et al., 2003 for details). We may assume that not more than 20 thermal pulses with dredge-up contribute to the envelope enrichment with *s*-process material ( $m = 20$ ).

By evaluating Eq. (1) for the numbers specified above we can derive a logarithmic expression that relates the average *s*-process overabundance in the PM zone with the mass of that zone:

$$\log M_{\text{PM}} = -[s/Fe]_{\text{PM}} + c \quad (2)$$

where  $Y_{\text{env}}$  in Eq. (1) is given by using  $[s/Fe]_{\text{env}} = 1$ , and  $c = -0.44$  for  $m = 20$ .

In Fig. 1 we show the variation of  $[s/Fe]_{\text{PM}}$  and  $[hs/lis]_{\text{PM}}$  with the neutron exposure in a *s*-process one-zone model. As more neutrons are released the average *s*-process overabundance  $[s/Fe]_{\text{PM}}$  increases. The partial mixing zone should not extend into the He-shell. This puts a lower limit on  $[s/Fe]_{\text{PM}}$  and thus on the neutron exposure in the partial mixing zone. In Fig. 1 the dashed horizontal line corresponds to  $M_{\text{PM}} < 10^{-2} M_{\odot}$  and  $c = -0.44$ , and according to Eq. (2)  $[s/Fe]_{\text{PM}}$  above that line are allowed. From  $[hs/lis]_{\text{obs}} < 0.0$  (dotted line) it follows that the neutron exposure should not exceed  $\sim 0.45 \text{ mbarn}^{-1}$  in the partial mixing zone. Otherwise the envelope *s*-process abundance distribution will eventually be top-heavy as well, and not in agreement with observations (Lugaro et al., 2003).

Thus, we estimate that the neutron exposure at the end of the interpulse phase should be in the range  $0.25 \text{ mbarn}^{-1} < \tau < 0.45 \text{ mbarn}^{-1}$ . Using Eq. (2) and  $[s/Fe]_{\text{PM}} = 4.0$  at the upper  $\tau$  limit, the mass of the partial mixing zone should obey  $\log M_{\text{PM}} > -4.44$  (assuming  $m = 20$ ). These estimates are roughly in agreement with the much more detailed analysis of the partial mixing zone by Gallino et al. (1998).

### 3. *s*-Process Nucleosynthesis in a Rotating AGB Model Star

Rotation induces mixing in stars through a variety of processes (Maeder & Meynet, 2000). In rotating AGB stars a large angular velocity gradient develops at the interface of the compact and fast rotating core and the slow rotating envelope. For our analysis we take the corresponding mixing efficiencies and thermodynamic input from a  $3 M_{\odot}$  stellar model sequence including rotation (Langer et al., 1999). These models predict that shear mixing is continuously present at the core-envelope interface throughout the interpulse phase. For the *s*-process the effective Lagrangian mixing efficiency is important. Note, that

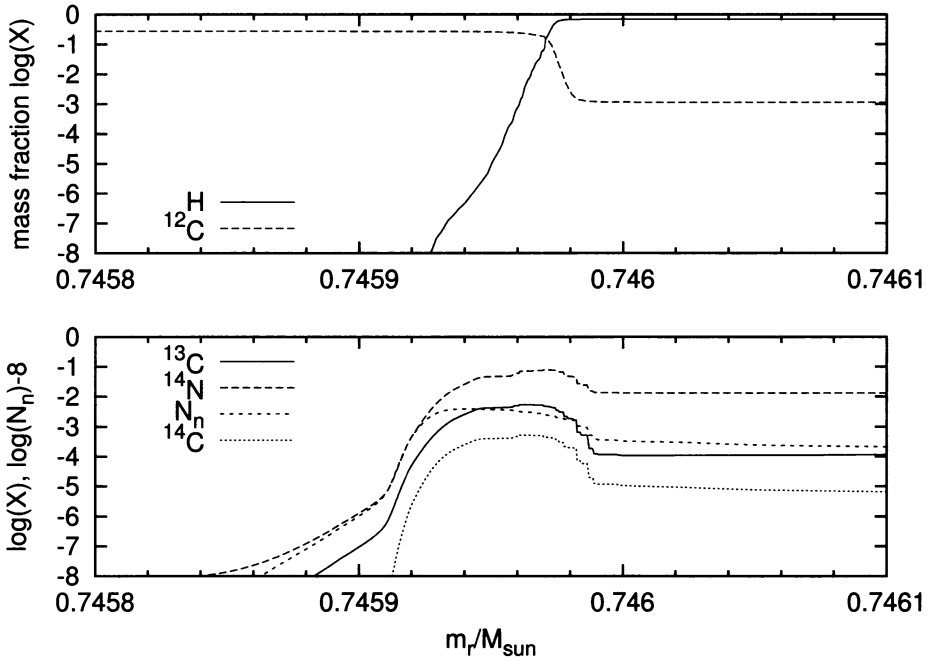


Figure 2. Abundance profiles in the partial mixing zone immediately after the end of the dredge-up phase (upper panel) and when the  $^{13}\text{C}(\alpha, n)^{16}\text{O}$  reaction is activated (lower panel).

the partial mixing layer is contracting significantly during the interpulse phase. Around the time of  $^{13}\text{C}(\alpha, n)^{16}\text{O}$  ignition (interpulse phase  $\phi \sim 0.3$ ), the diffusion coefficient is  $D_{\text{rot}} \sim 10^{-13} M_{\odot}/\text{yr}$ , which gives for a mixing timescale of  $\sim 1000$  yr a mixing range of  $\sim 10^{-5} M_{\odot}$ .

We use our *nuclear network and mixing post-processing* code to evaluate the effect of mixing on the *s*-process. This code solves simultaneously for mixing processes and all considered nuclear processes (charged particle reactions, neutron captures and  $\beta$ -decays). In the network all relevant charged particle reactions from hydrogen to  $^{31}\text{P}$  have been considered with rates mainly taken from Angulo et al. (1999). Neutron captures for 15 light isotopes and 9 iron group species have been considered and most cross sections are from Bao et al. (2000). The neutron capture on species beyond  $^{60}\text{Ni}$  are considered by a two step heavy neutron sink. We introduce two artificial particles ( $^{63}\text{G}$  and  $^{1}\text{L}$ ) with two extra reactions ( $^{62}\text{Ni}(n, \gamma)^{63}\text{G}$  and  $^{63}\text{G}(n, ^1\text{L})^{63}\text{G}$ ) which together give an estimate on *s*-process efficiency. For the Maxwellian averaged neutron capture cross section of  $^{63}\text{G}$  we take  $\sigma_{63\text{G}}(8\text{keV}) = 120$  mbarn, which has been determined from extensive one-zone model tests with a full *s*-process network.

In Fig. 2 we show the abundance profiles around the core boundary at two times of the post-processing calculation of one interpulse phase of the model sequence with rotation. The top panel shows the initial condition where rotationally induced mixing has caused some diffusion of protons into the  $^{12}\text{C}$  rich

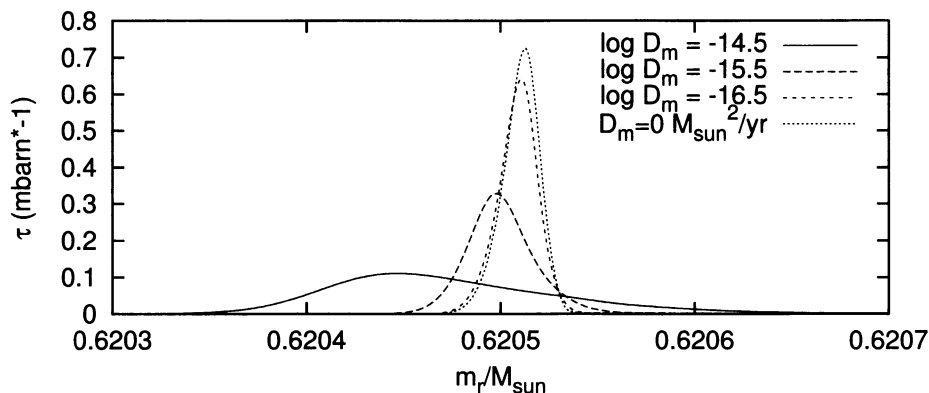


Figure 3. Final neutron exposure at the end of the interpulse for different assumptions on mixing. All cases start with a  $\text{H}/^{12}\text{C}$  partial mixing zone from hydrodynamic overshooting. During the interpulse no mixing (dotted line) and constant Lagrangian mixing coefficients have been applied ( $D_m$  in units of  $M_\odot/\text{yr}$ ).

core at the end of the (in this case shallow) third dredge-up. Goriely & Mowlavi (2000) have shown that in such a situation of a continuously decreasing proton abundance profile into the  $^{12}\text{C}$  rich core the mass range with a proton abundance of  $-2 < \log X_p < -3$  will eventually host *s*-process enriched material. According to this criterion, and given the required properties of the partial mixing zone as estimated in the previous section the partial mixing zone obtained in this rotating model is too thin.

The lower panel of Fig. 2 shows the situation when neutrons are beginning to be released by the  $^{13}\text{C}(\alpha, n)^{16}\text{O}$  reaction. In models without rotation, where the partial mixing zone results for example from hydrodynamic overshooting, the  $^{14}\text{N}$  and the  $^{13}\text{C}$  pocket keep mainly separated. With rotation instead the  $^{14}\text{N}$  abundance exceeds that of  $^{13}\text{C}$  in the entire partial mixing zone.  $^{14}\text{N}$  is an efficient neutron absorber, most notably through the  $(n, p)$  reaction. The recycling effect of the protons released in this reaction and the subsequent  $^{12}\text{C}(p, \gamma)^{13}\text{C}$  reaction does not balance the poison effect of  $^{14}\text{N}$ . As a result the neutron densities are low and the final maximum neutron exposure is much lower ( $\tau \sim 0.04 \text{ mbarn}^{-1}$ ) than our estimates from the previous section require.

#### 4. Parametric Models and Discussion

It seems that current models of rotation in AGB stars predict interpulse mixing coefficients that could inhibit the *s*-process during the interpulse phase due to dilution of the  $^{13}\text{C}$  pocket and admixture of the neutron poison  $^{14}\text{N}$ . In order to further study the effect of mixing during the interpulse we have constructed some parametric *s*-process models assuming a constant diffusive mixing coefficient  $D_m$  in Lagrangian coordinates during the interpulse phase. We start in all cases with abundance profiles at the core-envelope interface shaped by hydrodynamic overshooting as described in Herwig (2000). The final neutron exposure at the

end of the interpulse phase is shown in Fig. 3 for several cases. The case without mixing shows a larger neutron exposure than allowed according to the estimates in §2. For the cases with constant  $D_m$  we find an anti-correlation of mixing efficiency and final neutron exposure. Mixing coefficients over a range of two orders of magnitude correspond to a large spread of neutron exposure. For larger mixing efficiencies the pocket containing *s*-process enriched material becomes broader. However, the mixing coefficients that reproduce neutron exposures estimated in §2 are much smaller than what is predicted by the full stellar evolution model with rotation. We attempt to attribute this to unaccounted processes of angular momentum transport like magnetic fields (see Heger et al., these proceedings) in the AGB models. The simple parametric models indicate a possible solution for the apparent spread in *s*-process efficiency reported from pre-solar grains (Lugaro et al., 2003a) as well as from AGB and post-AGB stellar observations (Van Winckel & Reyniers, 2000; Busso et al., 2001).

**Acknowledgements:** F.H. would like to thank D.A. Vandenberg for support through his Operating Grant from the Natural Science and Engineering Research Council of Canada.

## References

- Angulo, C., Arnould, M., & Rayet, M. et al. 1999, Nucl. Phys., A 656, 3, NACRE compilation
- Bao, Z. Y., Beer, H., Käppeler, F., Voss, F., Wisshak, K., & Rauscher, T. 2000, ADNDT 76, 70
- Busso, M., Gallino, R., Lambert, D. L., Travaglio, C., & Smith, V. V. 2001, ApJ 557, 802
- Busso, M., Gallino, R., & Wasserburg, G. J. 1999, ARA&A 37, 239
- Busso, M., Lambert, D. L., Beglio, L., Gallino, R., Raiteri, C. M., & Smith, V. V. 1995, ApJ 446, 775
- Gallino, R., Arlandini, C., Busso, M., Lugaro, M., Travaglio, C., Straniero, O., Chieffi, A., & Limongi, M. 1998, ApJ 497, 388
- Goriely, S. & Mowlavi, N. 2000, A&A 362, 599
- Herwig, F. 2000, A&A 360, 952
- Herwig, F., Langer, N., & Lugaro, M. 2003, ApJ 593, 1056
- Langer, N., Heger, A., Wellstein, S., & Herwig, F. 1999, A&A 346, L37
- Lugaro, M., Davis, A. M., Gallino, R., Pellin, M. J., Straniero, O., & Käppeler, F. 2003a, ApJaccepted
- Lugaro, M., Herwig, F., Lattanzio, J. C., Gallino, R., & Straniero, O. 2003b, ApJ in press
- Maeder, A. & Meynet, G. 2000, ARA&A 38, 143
- Van Winckel, H. & Reyniers, M. 2000, A&A 354, 135